

Neutrophil-derived cathelicidin promotes cerebral angiogenesis after ischemic stroke

Journal of Cerebral Blood Flow & Metabolism
2023, Vol. 43(9) 1503–1518
© The Author(s) 2023
Article reuse guidelines:
sagepub.com/journals-permissions
DOI: 10.1177/0271678X231175190
journals.sagepub.com/home/jcbfm



Wanqing Xie*, Tingting Huang*, Yunlu Guo*, Yueman Zhang, Weijie Chen, Yan Li, Chen Chen and Peiyong Li 

Abstract

Neutrophils play critical roles in the evolving of brain injuries following ischemic stroke. However, how they impact the brain repair in the late phase after stroke remain uncertain. Using a prospective clinical stroke patient cohort, we found significantly increased cathelicidin antimicrobial peptide (CAMP) in the peripheral blood of stroke patients compared to that of healthy controls. While in the mouse stroke model, CAMP was present in the peripheral blood, brain ischemic core and significantly increased at day 1, 3, 7, 14 after middle cerebral artery occlusion (MCAO). CAMP^{-/-} mice exhibited significantly increased infarct volume, exacerbated neurological outcome, reduced cerebral endothelial cell proliferation and vascular density at 7 and 14 days after MCAO. Using bEND3 cells subjected to oxygen-glucose deprivation (OGD), we found significantly increased angiogenesis-related gene expression with the treatment of recombinant CAMP peptide (rCAMP) after reoxygenation. Intracerebroventricular injection (ICV) of AZD-5069, the antagonist of CAMP receptor CXCR2, or knockdown of CXCR2 by shCXCR2 recombinant adeno-associated virus (rAAV) impeded angiogenesis and neurological recovery after MCAO. Administration of rCAMP promoted endothelial proliferation and angiogenesis and attenuated neurological deficits 14 days after MCAO. In conclusion, neutrophil derived CAMP represents an important mediator that could promote post-stroke angiogenesis and neurological recovery in the late phase after stroke.

Keywords

Ischemic stroke, neutrophil, cathelicidin, cerebral endothelial cell, angiogenesis

Received 11 January 2022; Revised 10 March 2023; Accepted 9 April 2023

Introduction

Cerebral ischemic stroke, as the leading cause of morbidity and mortality worldwide,¹ causes cerebral blood flow reduction and blocks the oxygen and nutrients supply to the ischemic brain, ultimately causing cell death and tissue damage. In response to the ischemic injury, the brain adapts to compensate for the insufficient oxygen supply and angiogenesis takes place as early as 3 days after stroke, thus promoting the rebuilding of blood flow to support neurological recovery.² Recent studies suggest that immune cells and cytokines fundamentally participate in the regulation of angiogenesis, which provides a novel immunological insight for stroke recovery treatment.³

Neutrophils are the most abundant innate immune cell type that can be recruited from peripheral blood and

infiltrated into the ischemic brain early after stroke.^{4,5} It has been long recognized as the major pro-inflammatory immune cells that play critical roles in the evolving of neuroinflammation after stroke.^{6–8} However, recent evidence is emerging that neutrophils may

Department of Anesthesiology, Key Laboratory of the Ministry of Education of Anesthesia Medicine, Clinical Research Center, Renji Hospital, Shanghai Jiao Tong University School of Medicine, Shanghai, China

*These authors contributed equally to this work.

Corresponding author:

Peiyong Li, Department of Anesthesiology, Clinical Research Center, Renji Hospital, Shanghai Jiao Tong University School of Medicine, 160 Pujian Rd, Shanghai 200127, China.
Email: peiyongli.md@gmail.com

promote tissue repair after ischemic diseases.^{4,9–11} ECs are the first stop of peripheral neutrophils that adhere to the brain vasculature following ischemic stroke and can attract neutrophils by expressing a variety of cytokines and chemokines.^{12–14} However, whether and how neutrophils affect the proliferation of ECs and promote brain repair in the delayed stroke-damaged brain remains unknown.

The cathelicidin antimicrobial peptide (CAMP) is derived from neutrophils by de-granulation.¹⁵ Previous studies have shown that CAMP promotes wound healing by stimulating epithelialization and angiogenesis of injured tissue.^{16–18} The pro-healing effects of CAMP can be mediated by altering growth factor/receptor interactions.^{19,20} In addition, CAMP can induce angiogenesis through prostaglandin E₂-EP3 signaling in endothelial cells,¹⁸ or formyl peptide receptor-like 1 expressed on endothelial cells.¹⁷ The above evidences suggest that CAMP plays an important role in regulating the proliferation of ECs.

In this study, we find that neutrophil-derived CAMP promotes the proliferation of cerebral ECs and angiogenesis, partially through CXCR2 receptor on ECs. We propose that CAMP could be a potent pro-angiogenesis factor, which may serve as a therapeutic target to promote cerebral blood flow reconstruction and improve neurological function in the late phase of ischemic stroke.

Materials and methods

Animals

Adult male C57BL/6 mice (6–8 weeks) were purchased from Shanghai Jiesijie Laboratory Animal Co., Ltd and were housed in a standard laboratory room (12-h light/dark cycle, constant temperature and humidity controlled, with free access to food and water). CAMP^{-/-} mice were purchased from the Cyagen Biosciences Co., Ltd. All mice were bred on a C57BL/6 background. All animal experiments were approved by the Renji Hospital Institutional Animal Care and Use Committee and performed in accordance with the Institutional Guide for the Care and Use of Laboratory Animals. Animal data reporting followed the ARRIVE 2.0 guidelines.²¹

Middle cerebral artery occlusion model (MCAO)

Cerebral ischemia was induced by intraluminal occlusion of the left middle cerebral artery (MCA). Mice were anesthetized with 2% isoflurane in 70% N₂/30% O₂. Body temperature was maintained constantly at 37–37.5°C with a heating pad. A silicone-coated filament was advanced through the left internal carotid

artery until it occluded the MCA. After 60 minutes MCAO, the filament was removed to allow reperfusion.

Cerebral blood flow measurement

Cerebral blood flow (CBF) was measured with a laser speckle contrast imaging (LSCI). CBF measurements were performed under anesthesia with 2% isoflurane. CBF values were assessed using regions of interests (ROIs) on ipsilateral and contralateral sides of the MCA areas. The images were recorded while the body temperature, heart rate was stably maintained for 1 min. The mean values from 15 perfusion images were chosen for quantification.²²

Assessments of neurological deficit

The evaluation of neurological deficit was performed on 1, 3, 5, 7, 14 days after MCAO by investigators blinded to experimental group assignments.

Rotarod. Mice were placed on the rotating rod (YLS-4D) of 3.0 cm diameter, and trained to stay on the rod for 300 sec in an accelerated speed from 5 rpm to 40 rpm. The latency to fall or spin around on the rungs was recorded.

Foot-fault test. Each mouse was placed on a steel grid floor (20 cm × 40 cm with a mesh size of 4 cm²) elevated 50 cm above the floor and videotaped. The number of errors (when the mouse misplaced forelimb and fell through the grid) was recorded for a 5-minute-long observation period.

Garcia score. The modified Garcia score system was established to evaluate sensorimotor function. The score consists of 5 tests: body proprioception, vibrissae touch, limb symmetry, climbing, and forelimb walking with scores of 0–3 for each test (maximum score of 15).

Neutrophil depletion

Neutrophils were depleted using anti-Ly6G mAb (#BE0075-1, BioXCell).²³ Specifically, starting at 1 day before MCAO and 1, 3, 5, 7 days after MCAO, mice were injected i.p. with anti-Ly6G mAb (0.1 mg/day) to deplete neutrophils or with rat IgG (BP0089, BioXCell) as control. The efficiency of neutrophil depletion in MCAO mice was confirmed by flow cytometry.

Immunofluorescence

Mice were intravenously injected with Lycopersicon esculentum (Tomato) Lectin (LEL, TL), DyLight 594 (300 ug/mL, Invitrogen, L32471) four hours before

sacrificed. Coronal sections were incubated with 10% normal donkey serum for 60 minutes at room temperature in PBS containing 0.3% Triton X-100 (0.3% PBST) followed by incubation with appropriate primary antibodies overnight at 4 °C in the same buffer. The anti-CAMP (1:500, Novus), anti-CD31 (1:500, R&D), anti-NeuN (1:500, Abcam), anti-GFAP (1:500, Abcam), anti-Iba1 (1:500, Abcam), anti-Map2 (1:500, Abcam), anti-ZO-1 (1:500, Abcam), anti-CXCR2 (1:500, Abcam), anti-myeloperoxidase (1:500, Abcam) primary antibodies were used. Sections were then washed three times with 0.3% PBST followed by incubation with appropriate fluorescent-labeled secondary antibodies (1:500) for 2 hours at room temperature. DAPI was incubated for counterstaining of the nucleus. All immunofluorescence images were captured on a laser scanning confocal microscope (Olympus Fluoview FV3000, Olympus).

Image acquisition and analysis

EdU images were analyzed manually by using NIH Image J (1.52a). TIFF files were converted into binary images by setting a fixed threshold for both CD31 and EdU signal intensity, merged edged of close nuclei were split through the Watershed plug-in and nuclei count was performed with the built-in particle analysis plug-in. Accepted nuclei dimension were set in a range corresponding to the second and third quartiles of all particles detected. Three randomly selected microscopic fields in the cortex on each section were analyzed for each brain by a blinded investigator. The immune-positive cells were presented as the mean numbers or percentage of cells per field.

Mean fluorescent intensity (MFI) is the mean of the fluorescence intensity in the fluorescence channel (Alexa 488, etc.). The MFI of CAMP, ZO-1 or CXCR2 in each section were averaged using NIH Image J (1.52a). $MFI(\text{Mean}) = \text{sum of fluorescence intensity in the region} / (\text{IntDen}) / \text{Area of the region} (\text{Area})$

Lectin-stained vessels were imaged with a confocal Olympus FV3000. Confocal images were processed to create maximum Z projections and saved as TIFF files before analysis. We use Vessel Analysis (Fiji) plugin to analyze the vascular density. Vessel Analysis is a plugin to automatically calculate vascular density metrics: vascular density = vessel area/total area $\times 100\%$ - vascular length density = skeletonized vessel area/total area $\times 100\%$. Three randomly selected microscopic fields in the cortex on each section were analyzed for each brain by a blinded investigator.

Flow cytometry

For peripheral blood cells, single cell suspensions were prepared using RBC lysis buffer (BD). Isolated cells

were stained with CD45-APC-Cy7 (ebioscience, USA), CD11b-PE (BD), Ly6G-BV421 (R&D), hCAP18-647 (Abcam). Flow cytometry was performed on BD FACSVerser (BD Bioscience). Data analysis was performed using FlowJo software (TreeStar).

Recombinant CAMP peptide (rCAMP) and antagonist delivery by intracerebroventricular (ICV) injection

rCAMP (Bioss, Y-0430) (2 mg/kg),^{24,25} CAMP receptor antagonist: AZD-5069 (MCE, HY-19855) (10 mg/kg)²⁶ and JNJ-47965567 (MCE, HY-101418) (10 mg/kg)²⁷ were delivered via ICV injection 4 hours after reperfusion. ICV administration was performed as previously described.²⁸ A 1-mm cranial burr hole was drilled at the following coordinates relative to bregma: 0.22 mm posterior, 1.0 mm lateral. A 26-gauge needle of a 10 μL Hamilton syringe was inserted into the left lateral ventricle through the cranial burr hole at the depth of 2.25 mm deep under dura. A micro-infusion pump was used for ICV injection at a rate of 1 $\mu\text{L}/\text{min}$. The needle was left in place for an additional 5 min at the end of infusion and then removed slowly during a 3-min period.

Oxygen glucose deprivation (OGD)

An *in vitro* OGD model was established as previously described.²⁹ Briefly, the culture media of bEND3 cells were replaced with OGD media, composed of DMEM with no glucose or serum. Cells were then transferred to a humidified hypoxia chamber flushed with OGD gas mixture (95% N_2 , 5% CO_2). The oxygen level was kept constant at approximately 0.3% throughout the duration of the experiment by a digital oxygen controller (Biospherix). Glucose containing media was applied 6 h after OGD to achieve reoxygenation.

RNA sequencing

The total RNA was extracted using RNeasy Mini Kit (Cat#74106, Qiagen), and RNA quality was checked using an Agilent Bioanalyzer 4200 (Agilent technologies, Santa Clara, CA, US). Sequencing libraries were generated using VAHTS Stranded mRNA-seq Library Prep Kit for Illumina (NR612, Vazyme, Nanjing, China) according to the manufacturer's instructions. The sequencing was performed on Illumina Nova seq platform (Illumina, San Diego, CA, USA). Genes with $P\text{-value} < 0.05$ and $|FC| > 2$ were considered as differentially expressed genes (DEGs). In order to understand the biological function of differentially expressed genes, we performed enrichment analysis based on the Gene Ontology (GO) database.

5-Ethynyl-2'-deoxyuridine(EdU) assay and cell proliferation

In vitro: 50 nM EdU reagent (Beyotime, C0078L) was added into 24-well plate seeded with bEND3 cells and incubated for 24 hours at 37 °C, then tested with flow cytometry. EdU incorporation and detection were performed as described by the manufacturer's protocol. Briefly, 100 μ L of 2 \times working solution of EdU was added to the wells with bEND3 cells in the 24-well plate during the exposure time for 24 hours with different rCAMP concentrations or CAMP antagonist. After incubation, the cells were fixed with 4% paraformaldehyde for 15 min and then 0.3% TritonX-100 with Phosphate Buffer Solution (PBST) for 15 mins at room temperature. The cells in each well were washed twice with 0.3% PBST between every two steps. Then, 100 μ L of click reaction cocktail was added to each well for 30 min and protected from light. Each well was washed twice with PBS. Flow cytometry was performed on BD FACSVerser (BD Bioscience). Data analysis was performed using FlowJo software (TreeStar).

In vivo: To label newly generated cerebral endothelial cells *in vivo* after ischemia, C57BL/6 mice were intraperitoneally injected with EdU (20 mg/kg) at 2 h, 1, 3, 5, 7 days after MCAO. Mice were sacrificed 4 hours after the last injection. EdU was detected using BeyoClick™ EdU Cell Proliferation Kit with Alexa Fluor 488 (Beyotime, C0071S).

Enzyme-linked immunosorbent assay

CAMP serological testing was performed using the commercially available human or mouse CAMP enzyme-linked immunosorbent assay (ELISA) kit according to the manufacturer's instructions (E-Elabscience, EL-H2438c; Signalway antibody, EK11115-1).

CXCR2 knock-down with recombinant adeno-associated virus (rAAV)

In vivo gene knock-down was achieved by rAAV vectors. Cerebral endothelial cells specific CXCR2-shRNA rAAV (rAAV-Tie-EGFP-5'miR-30a-shRNA (Cxcr2) -3'-miR30a-WPREs, BR1) and scramble-shRNA rAAV (rAAV-Tie-EGFP-5'miR-30a-shRNA (scramble) -3'-miR30a-WPREs, BR1) were chemically synthesized by BrainVTA Co., Ltd (Wuhan, China). rAAV was diluted in phosphate-buffered saline (PBS) to 2×10^{11} genome copies/100 μ L. Mice were injected intravenously with 100 μ L CXCR2-shRNA or scramble-shRNA rAAV suspension three weeks prior to MCAO.

Statistical analysis

Sample sizes for animal studies were determined by power calculations for the primary parameter with mean differences and standard deviations based on pilot studies or the literature (power = 80%, $\alpha = 0.05$).³⁰ All statistics were performed using GraphPad Prism(v.9.0.0). Results were presented as mean \pm standard deviation (SD). The Kolmogorov-Smirnov normality test was initially performed on all datasets. For normally distributed continuous variables, comparisons between two groups were conducted by the two-tailed Student's t-test (equal variances) or Welch's *t* test (unequal variances), and comparisons between multiple groups were conducted by one-way analysis of variance (ANOVA) followed by with Bonferroni multiple comparisons test or two-way ANOVA. Differences in means across groups with repeated measurements over time were analyzed using repeated measures ANOVA. When the ANOVA showed significant differences, pairwise comparisons between means were tested by post hoc Bonferroni (comparisons between all conditions), Dunnett (all conditions compared with a control group). For continuous variables with non-normal distributions or non-continuous variables, the two-tailed Mann-Whitney U rank sum test was used. In all analyses, $p < 0.05$ was deemed statistically significant.

Results

Stroke increases CAMP in patients' circulating neutrophils and the mouse ischemic brain

In a prospective cohort of ischemic stroke patients within 3 days after stroke onset (Table S1, S2), we examined the level of CAMP in the peripheral plasma. We found CAMP was maintained at a low level in the plasma of healthy controls, whereas stroke led to a significant increase both in male and female patients within 3 days (Figure 1(a) and (b)). Using a mouse model of MCAO, we found the expression of CAMP in plasma significantly increased at 1, 3, 7 and 14 days after MCAO and the CAMP level peaked at 3 days after MCAO in male mice, but at 7 days after MCAO in female mice (Figure 1(c) and (d)). In addition, the number and percentage of CAMP⁺Ly6G⁺ neutrophils in the peripheral blood of MCAO mice were remarkably increased at 1 and 3 days after MCAO compared to that of the sham mice (Figure 1(e) to (i)). CAMP⁺ Ly6G⁺ neutrophils were also increased in the infarct core regions at 3, 7 and 14 days after MCAO as revealed by immunofluorescent staining (Figure 1(j) to (l)). We also found

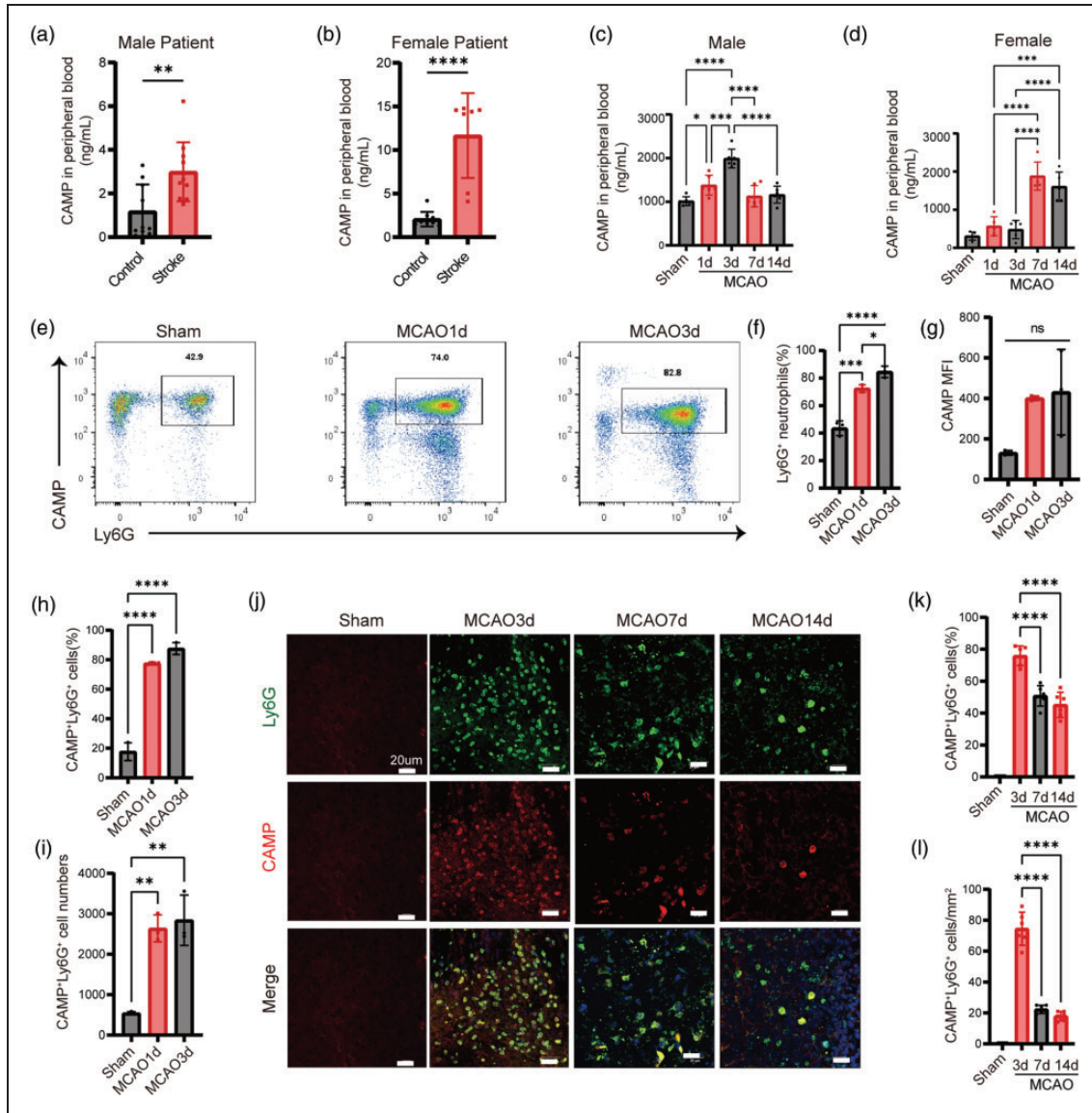


Figure 1. CAMP is upregulated in circulating neutrophils and ischemic brain. (a–b) Quantification of CAMP in the plasma of male (a) and female (b) stroke patients within 3 days by ELISA ($n = 17\text{--}23$ per group, unpaired Student's t -test). (c–d) Quantification of CAMP in the plasma of MCAO male mice (c) and female mice (d) at 1, 3, 7 and 14 days after MCAO ($n = 6$ per group, one-way ANOVA with Bonferroni multiple comparisons test). (e) Representative flow cytometry plots for $\text{CAMP}^+ \text{Ly6G}^+$ neutrophils in the peripheral blood of MCAO mice at 1 and 3 days after MCAO. (f–i) Quantification of $\text{CAMP}^+ \text{Ly6G}^+$ neutrophils cell numbers and percentage, total neutrophils percentage and CAMP MFI in the peripheral blood at 1 and 3 days after MCAO ($n = 3$ per group, one-way ANOVA with Bonferroni multiple comparisons test). (j) Representative images showed expression of CAMP in neutrophils infiltrated in the infarct core at indicated timepoints after MCAO. The representative pictures of three individual mouse samples per group were shown. Scale bar, $20\mu\text{m}$ and (k–l) Quantification of $\text{CAMP}^+ \text{Ly6G}^+$ neutrophils counts per mm^2 and percentage in the infarct core at indicated timepoints after MCAO ($n = 6$ per group, one-way ANOVA with Bonferroni multiple comparisons test). All data are presented as means \pm SD, * $P < 0.05$, ** $P < 0.01$, *** $P < 0.001$, **** $P < 0.0001$, ns, no significance.

CAMP^+ neutrophils in the peri-infarct region at 3, 7, 14 days after MCAO (Fig.S4A–B). These data suggest that stroke increases CAMP both in circulating neutrophils and the neutrophils infiltrated into the ischemic brain.

CAMP deficiency increases infarct volume and impairs neurological recovery after ischemic stroke

Given CAMP was exclusively expressed in neutrophils as revealed by Mariana et al,^{31,32} together with the secondary analysis of the single cell RNA sequencing

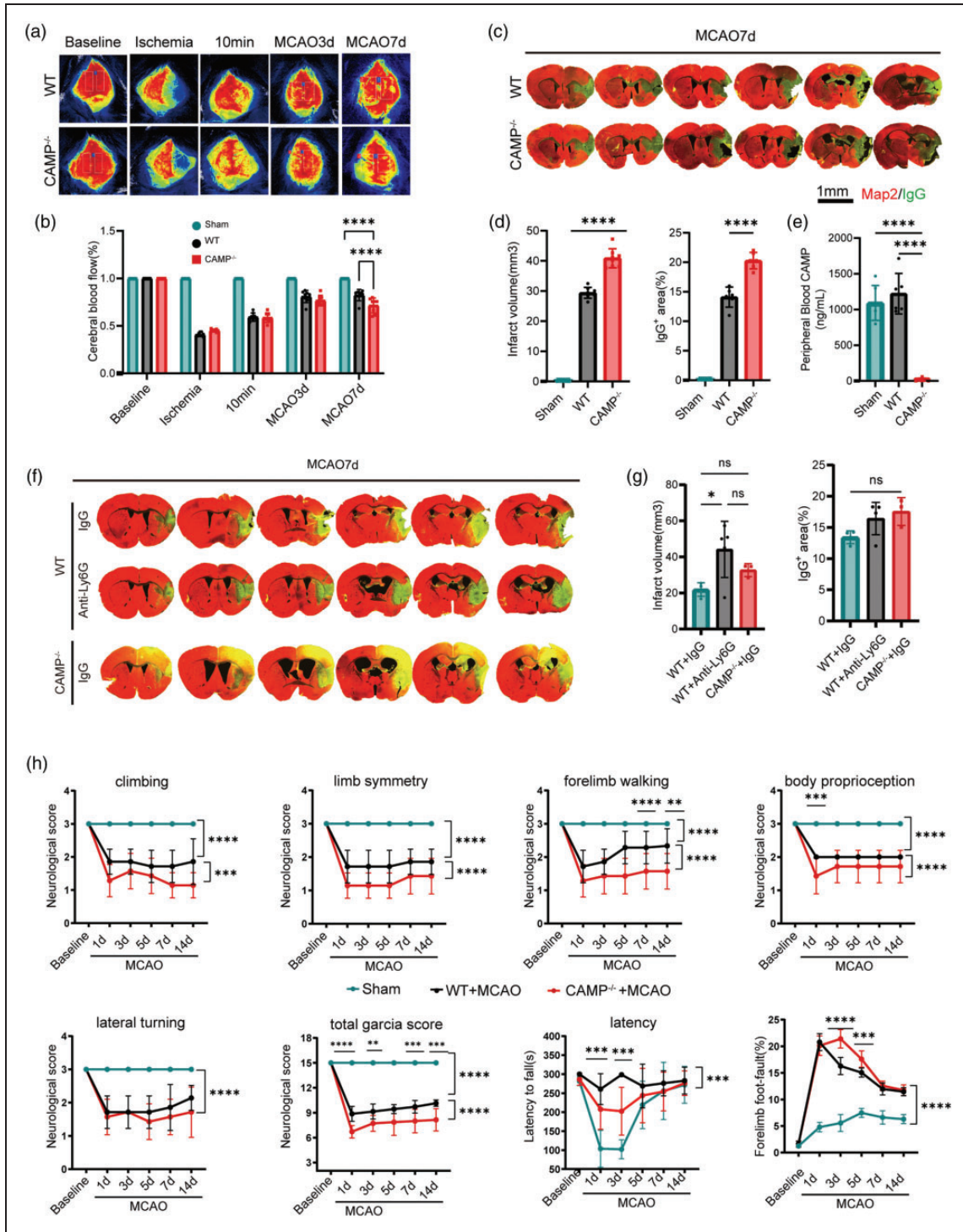


Figure 2. Neurophil-derived CAMP deficiency increases infarct volume and impairs neurological recovery after ischemic stroke. (a) Representative images of cerebral blood flow (CBF) of WT and $CAMP^{-/-}$ mice before MCAO (baseline), during ischemia, 10 minutes, 3 days and 7 days after reperfusion. (b) Quantitative measurements of CBF of Sham, WT and $CAMP^{-/-}$ mice at indicated timepoints. Results were expressed as percent change from baseline ($n = 8$ per group, one-way ANOVA with Bonferroni multiple comparisons test). (c) Representative MAP2 staining of brain infarct and endogenous mouse IgG staining of BBB leakage of WT and $CAMP^{-/-}$ mice 7 days after MCAO. Scale bar, 1 mm. (d) Quantification of infarct volume and endogenous IgG positive area of WT and $CAMP^{-/-}$ mice 7 days after MCAO ($n = 8$ per group, one-way ANOVA with Bonferroni multiple comparisons test). (e) Quantification of CAMP in the plasma of WT and $CAMP^{-/-}$ male mice 7 days after MCAO ($n = 6$ per group, one-way ANOVA with Bonferroni multiple comparisons test). (f) Representative MAP2 staining of brain infarct and endogenous mouse IgG staining of BBB leakage of WT and $CAMP^{-/-}$ mice 7 days after MCAO. (g) Quantification of infarct volume and endogenous IgG positive area of WT and $CAMP^{-/-}$ mice 7 days after MCAO. (h) Neurological recovery scores for climbing, limb symmetry, forelimb walking, body proprioception, lateral turning, total garcia score, latency, and forelimb foot-fault percentage over time. Continued.

dataset (GSE174574), which suggested that CAMP expressed mainly in neutrophils³³ (Fig. S2B), we next used CAMP knock-out mice (CAMP^{-/-}) to examine the role of neutrophil-derived CAMP in ischemic brain injury, we found that the CBF of CAMP^{-/-} mice was lower than WT mice at 7 days after MCAO (Figure 2(a) and (b)). In addition, compared to WT mice, CAMP^{-/-} mice exhibited significantly increased infarct volume, aggravated BBB damage as quantified by the extravasation of plasma-derived IgG 7 days after MCAO (Figure 2(c) to (e)). We next compared the above parameters in the neutrophil depleted mice with those in the CAMP^{-/-} mice. We found neutrophil depletion successfully reduced the neutrophil counts and CAMP peptide in the peripheral blood of WT mice 7 days after MCAO (Fig.S1A-D). In addition, sustained depletion of neutrophils until late phase increased infarct volume with the extent similar to CAMP^{-/-} mice (Figure 2(f) to (g)). In terms of the neurological function after MCAO, we found that the modified Garcia score and time-to-fall off an accelerating rotating rod (rotarod test)³⁴ were both significantly decreased in the CAMP^{-/-} mice compared to the WT mice 7 days after MCAO (Figure 2 (h)). In the grid-walking test, the percentage of forelimb foot fault (right impaired forelimb foot fault/total amount of right forelimb step) were significantly higher in CAMP^{-/-} mice compared to WT mice (Figure 2(h)) during 14 days after MCAO. These results suggested that CAMP deficiency in neutrophils increased infarct volume and impaired late-phase neurological recovery after ischemic stroke.

CAMP promotes proliferation of cerebral ECs and angiogenesis following OGD in vitro and ischemic stroke in vivo

To examine the mechanism underlying the protective role of CAMP in the ischemic brain injury, we subjected bEND3 cells to OGD for 6 hours, and treated with rCAMP (5 µg/mL) or PBS for 24 hours after reoxygenation. We performed RNA sequencing on cell lysates of rCAMP or PBS treated bEND3 cells and found markedly changed transcriptional profile between the above two groups (Figure 3(a)). The gene expression heatmap revealed higher expression of angiogenesis-related genes such as vascular endothelial growth factor B (Vegfb), vasohibin 1 (Vash1), and catenin beta 1 (Ctnnb1) in rCAMP treated bEND3

cells compared to PBS group (Figure 3(b)). GO analysis on DEGs of rCAMP vs PBS group revealed enrichment in positive regulation of angiogenesis (GO:0045766) and vasculature development (GO:1904018) (Figure 3(c)). In addition, we found significantly decreased ZO-1 and lectin⁺ vascular density in the brain of CAMP^{-/-} mice compared to that of WT mice (Figure 2(d) to (g)). To validate the pro-angiogenic effect of CAMP after stroke, we examined the cerebral ECs' uptake of EdU after intraperitoneal injection of EdU 2 hours, 1, 3, 5 and 7 days following MCAO. We found a significant decrease in the number of Ki67⁺ or EdU⁺ nuclei within cerebral ECs from CAMP^{-/-} mice compared to those from WT mice 7 and 14 days after MCAO (Figure 2(h) to (i), Fig.S3A). We also evaluated the proliferation of different cell types in neurovascular unit, and found significantly higher uptake of EdU in cerebral ECs compared to neurons, microglia, and astrocytes 7 days after MCAO (Fig.S3B-F). The above evidence supports that CAMP can promote cerebral EC proliferation and angiogenesis after ischemic stroke.

CAMP promotes cerebral EC proliferation after ischemic injury in vivo and in vitro

To explore how CAMP promotes the proliferation of cerebral ECs, we treated bEND3 cells with different concentrations (1, 5, 10, 100 µg/mL) of rCAMP for 24 hours after reoxygenation (Figure 4(a)). EdU⁺ cells were detected by flow cytometry (Figure 4(b)). The dose-response experiment determined that 5 µg/mL of CAMP peptide administrated for 24 hours after OGD was the optimal regimen promoting cell proliferation (Figure 4(c) and (d)). Thus, 5 µg/mL of CAMP was used in all subsequent experiments. Since CAMP could combine to multiple receptors, including purinergic receptor P2X7, CXC chemokine receptor 2 (CXCR2), and formyl-peptide receptor-2 (FPR2).³⁵⁻⁴¹ We thus treated bEND3 cells with 5 µg/mL rCAMP together with antagonists of the above three receptors, including: AZD-5069 (antagonist of CXCR2); JNJ-47965567 (antagonist of P2X7); WRW4 (antagonist of FPR2) for 24 hours after reoxygenation. We found that AZD-5069 (1 mM) and JNJ-47965567 (1 mM)²⁷ significantly inhibited EdU uptake of bEND3 cells 24 hours after 6 hour-OGD compared to the PBS treated bEND3 cells (Figure 4(e) and (f)), suggesting CAMP

Figure 2. Continued.

neutrophil depletion, IgG control and CAMP^{-/-} groups. (g) Quantification of infarct volume and endogenous IgG positive area of neutrophil depletion, IgG control and CAMP^{-/-} groups 7 days after MCAO (n = 3-5 per group, one-way ANOVA with Bonferroni multiple comparisons test) and (h) Sensorimotor function was assessed using Garcia score, rotarod, and foot-fault test for CAMP^{-/-} vs WT mice after MCAO (n = 8 per group, two-way repeated measures ANOVA and post hoc Dunnett's test). All data are presented as means ± SD, *P < 0.05, **P < 0.01, ***P < 0.001, ****P < 0.0001, ns, no significance.

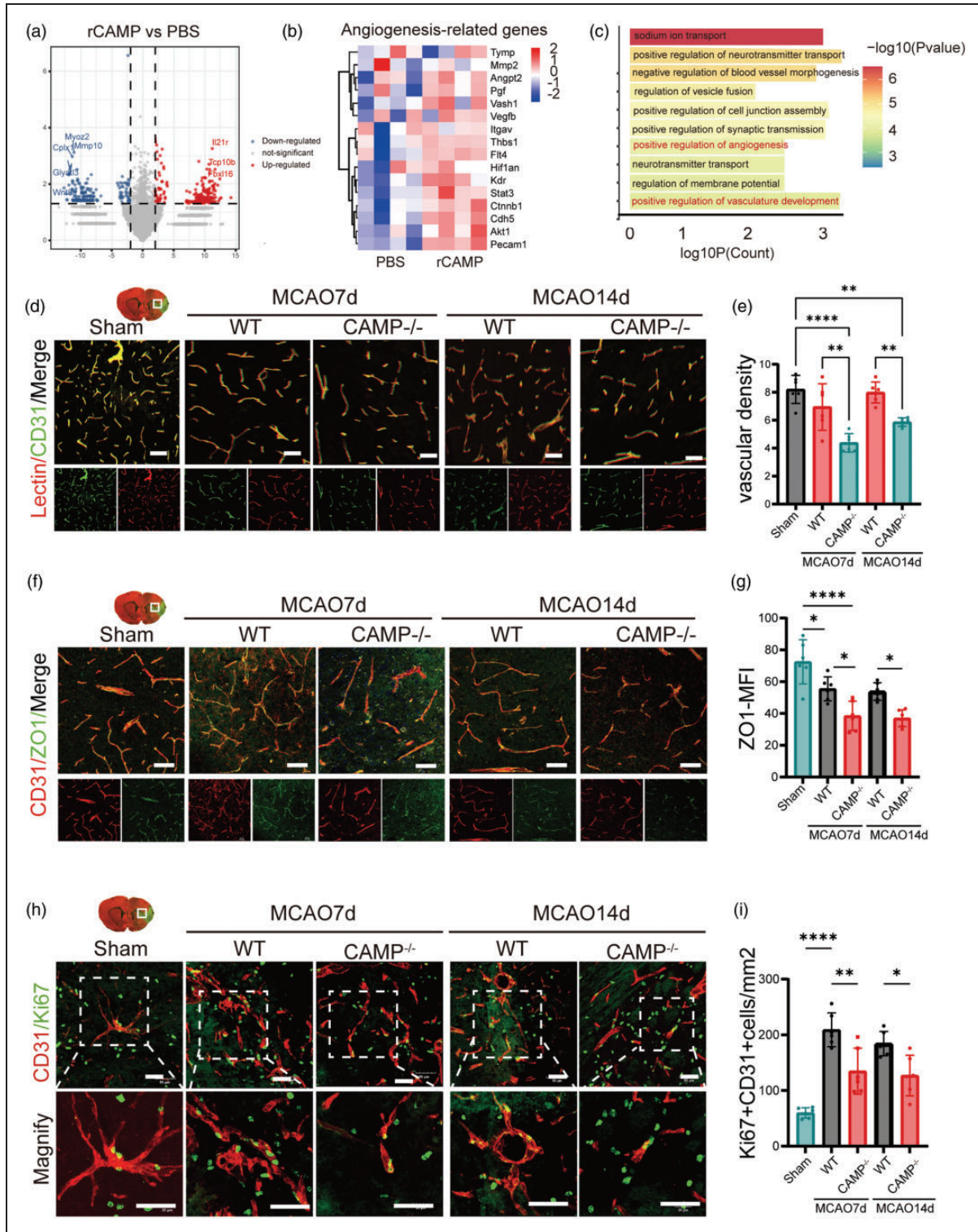


Figure 3. CAMP promotes proliferation of cerebral ECs and angiogenesis after ischemic stroke. (a) Volcano plot indicating transcriptomic changes between rCAMP and PBS group. (b) Heatmap showed the scaled expression of angiogenesis-related genes. (c) Bar plot showing the top enriched GO terms using the significantly upregulated genes in rCAMP treated bEND3 cells compared to PBS group. The color gradient indicates the number of genes per term. (d) Representative confocal images of lectin and CD31 double immunostaining in the penumbra regions of WT or *CAMP*^{-/-} mice 7 and 14 days after MCAO or sham surgery. Scale bar, 50µm. (e) Quantification of CD31⁺ lectin⁺ vascular density in the penumbra regions of WT or *CAMP*^{-/-} mice 7 and 14 days after MCAO or sham surgery (n = 6 per group, one-way ANOVA with Bonferroni multiple comparisons test). (f) Representative confocal images of
 Continued.

could induce proliferation of cerebral ECs by binding to CXCR2 receptor or P2X7 receptor. In order to further differentiate the receptor which is responsible for the EC proliferation following CAMP treatment *in vivo*, we treated mice with CXCR2 receptor antagonist AZD-5069 (10 mg/kg),²⁶ P2X7 receptor antagonist JNJ-47965567 (10 mg/kg)²⁷ or PBS *via* ICV injection 4 hours after MCAO. We found that compared to the PBS or JNJ-47965567 treated mice, AZD-5069 treated mice exhibited significantly increased infarct volume and aggravated BBB disruption 7 days after MCAO (Figure 4(g) to (i)), suggesting CXCR2 receptor could be the major receptor that mediated EC proliferation after rCAMP treatment in the delayed phase of stroke. In addition, the expression of CXCR2 receptor on CD31⁺ EC was significantly higher in the 14 days after MCAO (Figure 4(j) and (k)). In addition, we examined the infiltration of CAMP⁺Ly6G⁺ neutrophils in the ischemic brain of mice injected with vehicle or AZD-5069 (antagonists of CXCR2 receptor), and found no significant difference between the vehicle and AZD-5069 group in the peri-infarct area at 7 days after MCAO (Figure 4(l) and (m)).

CXCR2 mediates the CAMP associated angiogenesis and neurological recovery after ischemic stroke

In order to confirm that CAMP could promote angiogenesis and neurological recovery *via* CXCR2, we knockdown CXCR2 receptor of cerebral ECs specifically using rAAV *in vivo*. We found that compared to scramble-shRNA group, CXCR2-shRNA group exhibited increased infarct volume and aggravated BBB damage as quantified by the extravasation of plasma-derived IgG 7 days after MCAO (Figure 5(a) and (b)). Meanwhile, we detected significantly decreased ZO-1 density in the brain of CXCR2-shRNA group compared to that of scramble-shRNA group (Figure 5(c)). The CBF of CXCR2-shRNA group was lower than scramble-shRNA group at 3, 7 days after MCAO (Figure 5(d)). In addition, the modified Garcia score and time-to-fall off an accelerating rotating rod were both significantly decreased in the CXCR2-shRNA group compared to the scramble-shRNA group 7 days after MCAO (Figure 5(e)). Taken together, these data suggest that CAMP

promotes cerebral EC proliferation *via* binding to CXCR2 receptor.

rCAMP promotes cerebral EC proliferation and neurological repair after ischemic stroke

We next examined whether rCAMP could provide therapeutic effect to improve neurological recovery after ischemic stroke. We administered rCAMP (2 mg/kg) to the MCAO mice *via* ICV injection 4 hours, 1, 3, and 7 days after reperfusion²⁴ and found that rCAMP treated mice showed significantly reduced infarct volume as compared to the PBS treated mice 7 days after MCAO (Figure 6(c) and (d)). In addition, rCAMP treatment increased the density of CD31⁺ cerebral blood vessels and the number of CD31⁺EdU⁺ cells in the ischemic brain (Figure 6(e) to (h)). To examine the role of rCAMP treatment on the long-term neurological outcome, We found that the Garcia score of rCAMP treated mice were significantly higher than that of the PBS treated mice 14 days after MCAO. Meanwhile, time-to-fall off an accelerating rotating rod of the rCAMP treatment mice was significantly longer than that of the PBS treated mice 14 days after stroke (Figure 6(i)). Collectively, these data suggest that rCAMP treatment could induce cerebral EC proliferation, promote angiogenesis and attenuate neurological deficits during the late phase of stroke.

Discussion

In this study, we report, for the first time, that the host defensive peptide CAMP, released from neutrophils, promotes angiogenesis following ischemic stroke, which represents a novel therapeutic target to improve neurological recovery after stroke. The current finding proposes a novel neuroprotective role of neutrophils in the late phase of ischemic stroke.

CAMP, a cathelicidin-related antimicrobial peptide is generally considered to have anti-bactericidal effects.⁴² We measured the level of CAMP protein both in the peripheral blood of stroke patients and MCAO mice by ELISA. To further confirm the presence of CAMP in the ischemic brain, we detected CAMP⁺Ly6G⁺ neutrophils in the ischemic brain of MCAO mice. However, since we mainly focused the

Figure 3. Continued.

tight junction protein ZO-1 and CD31 in the penumbra regions of WT or CAMP^{-/-} mice 7 and 14 days after MCAO or sham operation. Scale bar, 50 μ m. (g) Quantification of ZO-1 MFI of CD31⁺ cerebral endothelial cells in the penumbra regions of WT or CAMP^{-/-} mice 7 and 14 days after MCAO or sham surgery (n = 6 per group, one-way ANOVA with Bonferroni multiple comparisons test). (h) Representative confocal images of CD31⁺ Ki67⁺ cells in the penumbra regions of WT or CAMP^{-/-} mice 7 and 14 days after MCAO or sham operation. Scale bar, 50 μ m and (i) Quantification of CD31⁺ Ki67⁺ cells in the penumbra regions of WT or CAMP^{-/-} mice 7 days after MCAO or sham surgery (n = 6 per group, one-way ANOVA with Bonferroni multiple comparisons test). All data are presented as means \pm SD, *P < 0.05, **P < 0.01, ***P < 0.001, ****P < 0.0001.

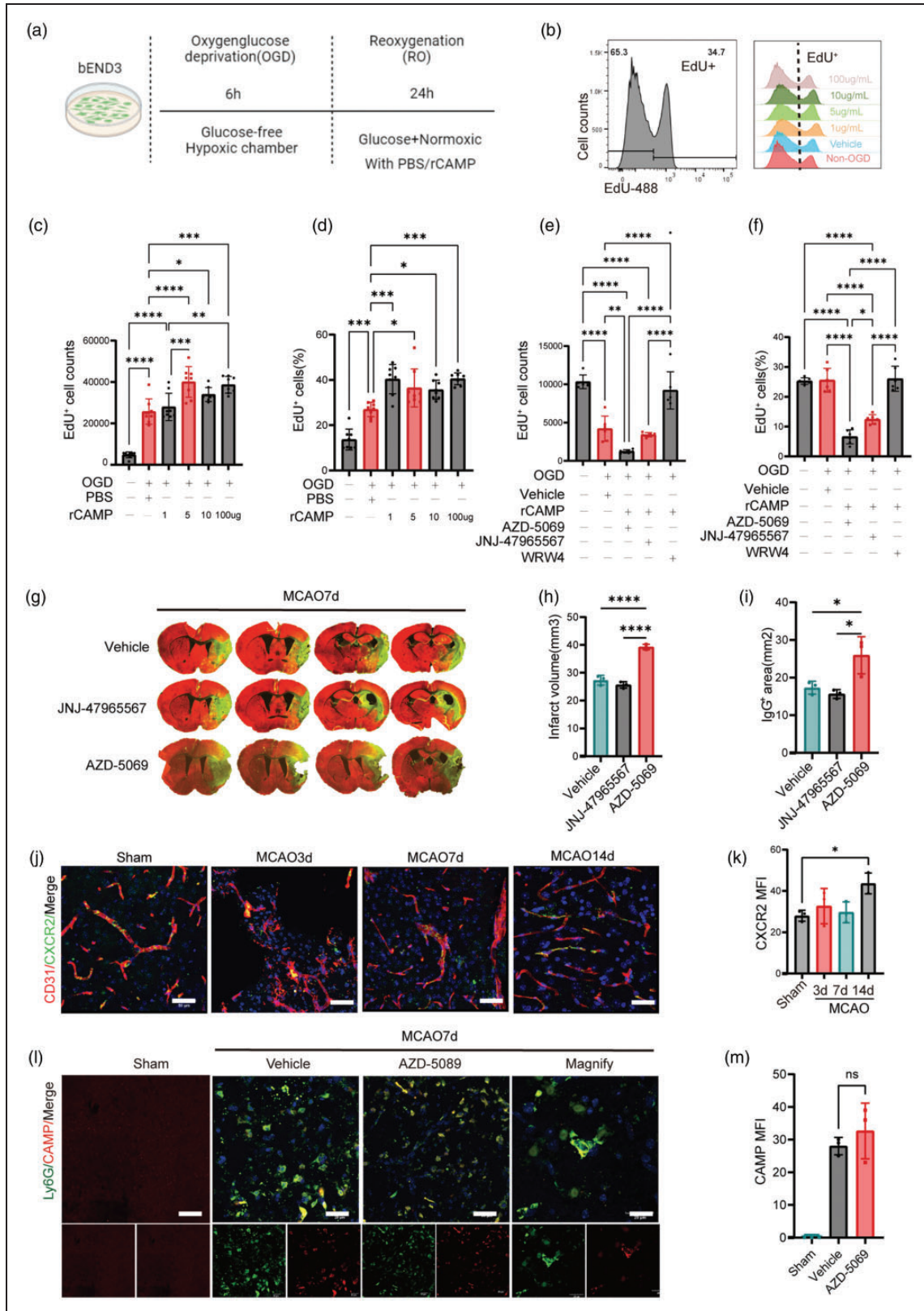


Figure 4. CAMP/CXCR2 mediated cerebral EC proliferation in vivo and in vitro after ischemic stroke. (a) Experimental design diagram. (b) Representative flow cytometry histogram of EdU⁺ bEND3 cells treated with different concentrations of rCAMP or vehicle after 6-hour OGD. (c–d) Quantification of EdU⁺ cell numbers (c) and percentage (d) treated with rCAMP concentration gradient of 1, 5, 10, 100µg/mL or vehicle after 6-hour OGD. (e–f) Quantification of EdU⁺ cell numbers (e) and percentage (f) treated with rCAMP concentration gradient of 1, 5, 10, 100µg/mL or vehicle after 6-hour OGD. (g–i) Quantification of infarct volume (h) and IgG area (i) in MCAO7d mice. (j–k) Immunofluorescence images (j) and CXCR2 MFI (k) in MCAO7d mice. (l–m) Immunofluorescence images (l) and CAMP MFI (m) in MCAO7d mice. Continued.

role of CAMP in the ischemic brain, the $\text{CAMP}^+\text{Ly6G}^+$ neutrophils in the peripheral blood of stroke patients were not examined. The current study demonstrated that CAMP regulated the proliferation of cerebral ECs and promoted angiogenesis, thus might serve as an important intrinsic mechanism that neutrophils promote brain repair after ischemic stroke. Our finding is consistent with the previous literature that showed CAMP were highly expressed during wound healing.⁴³

Angiogenesis is a critical step for functional recovery. When reperfusion is restored after transient ischemia, damage to the vascular endothelium and blood-brain barrier ensues, which represents one of the major mechanism underlying the no recurrent flow of blood vessels following revascularization therapy, such as thrombectomy and thrombolysis.^{44,45} According to the previous findings, new blood vessels start to appear on the 3rd day after stroke onset,⁴⁶ and angiogenesis is coupled with axonal outgrowth/neurogenesis, which together contribute to the functional recovery after cerebral ischemia.⁴⁷ In order to examine whether the angiogenesis induced by CAMP is functional *in vivo*, we injected *Lycopersicon esculentum* Tomato Lectin to mice intravenously 4 hours before sacrifice. The density of lectin-positive and CD31-positive cells (indicating functional blood vessels with blood flow perfusion) and CBF as measured by laser speckle contrast imaging of $\text{CAMP}^{-/-}$ mice were significantly lower than that of the WT mice at 7 days after MCAO.

Mechanistically, we found CAMP promoted angiogenesis by activating the CXCR2 receptor on cerebral ECs, while inhibition of CXCR2 suppressed CXCR2-promoted angiogenesis. The CXC chemokine receptor family belongs to the seven-transmembrane superfamily of G protein-coupled receptors.⁴⁸ CXCR2 is originally the high-affinity receptor on murine neutrophils, which is related to adhesion and rolling of neutrophils.⁴⁹ Interestingly, accumulating evidence suggests that CXCR2 expression is not only limited on neutrophils, but can also be found on other cells including endothelial cells. The interaction between CXCL/CXCR2 was considered to induce leukocyte migration,

angiogenesis and other functions.^{50,51} It was reported that CXCR2 on microvascular endothelial cells was activated by IL-8, which could contribute to the increased vascular permeability observed in acute inflammation and during the angiogenic response.⁵¹ In addition, CAMP may act as a functional ligand for CXCR2 on human neutrophils.⁴¹ The current study showed for the first time that CAMP released from neutrophils could promote angiogenesis by activating the CXCR2 receptor on cerebral EC in late phase of ischemic stroke.

In our study of the clinical cohort and the mice MCAO model, we found male and female mice exhibited remarkable difference in the CAMP peptide levels in the peripheral blood as examined by ELISA at indicated timepoints after stroke. The peak time of CAMP in male mice was 3 days after MCAO, while the peak of CAMP level in female mice was delayed until 7 days after MCAO.⁵² In human patients, the average level of CAMP in the peripheral blood of female was higher than that of men. It was previously shown that ovarian hormones could exert a potential effect on neutrophils, which could explain the CAMP discrepancy in neutrophils between genders.⁵³ For example, male neutrophils showed higher responsiveness to stimulation with LPS and $\text{IFN-}\gamma$ and higher expression of TLR4 compared to female neutrophils.⁵⁴ However, the gender difference of change in CAMP level has not been reported in literature so far, which needs further studies in this regard.

Despite the novelty of CAMP in angiogenesis in ischemic stroke, there were several limitations in our study. For example, the parameters examined for angiogenesis were relatively limited, such as the blood vessel density and the co-labeling of EdU, ZO-1, lectin and CD31^+ ECs. Another limitation of our study was that we were not able to distinguish the neurological deficits observed in $\text{CAMP}^{-/-}$ mice was due to exacerbated early brain injury or attenuated angiogenesis. Our results suggested that $\text{CAMP}^{-/-}$ mice had already showed subtle difference of neurological scores and behaviors from WT mice early after stroke. However, it was not specifically explored whether CAMP plays

Figure 4. Continued.

with rCAMP and CAMP receptor antagonist: AZD-5069, JNJ-47965567, WRW4 (1mM) or PBS after 6-hour OGD. (g) Representative MAP2 staining of brain infarct and endogenous mouse IgG staining of BBB leakage 7 days after MCAO in mice treated with AZD-5069, JNJ-47965567 or vehicle via ICV injection. (h–i) Quantification of infarct volume and endogenous IgG positive area of mice treated with AZD-5069, JNJ-47965567 and vehicle 7 days after MCAO ($n = 6$ per group, one-way ANOVA with Bonferroni multiple comparisons test). (j) Representative confocal images of CXCR2 and CD31 double immunostaining at 3, 7, 14 days after MCAO or sham operation. Scale bar, $50\mu\text{m}$. (k) Quantification of CXCR2 MFI of CD31^+ cerebral endothelial cells ($n = 3$ per group, one-way ANOVA with Bonferroni multiple comparisons test). (l) Representative confocal images of CAMP and Ly6G double immunostaining in mice injected with vehicle or AZD-5069 at 7 days after MCAO or sham operation. Scale bar, $20\mu\text{m}$. (m) Quantification of CAMP MFI in Ly6G^+ neutrophils ($n = 3$ per group, one-way ANOVA with Bonferroni multiple comparisons test). All data are presented as means \pm SD, * $P < 0.05$, ** $P < 0.01$, *** $P < 0.001$, **** $P < 0.0001$.

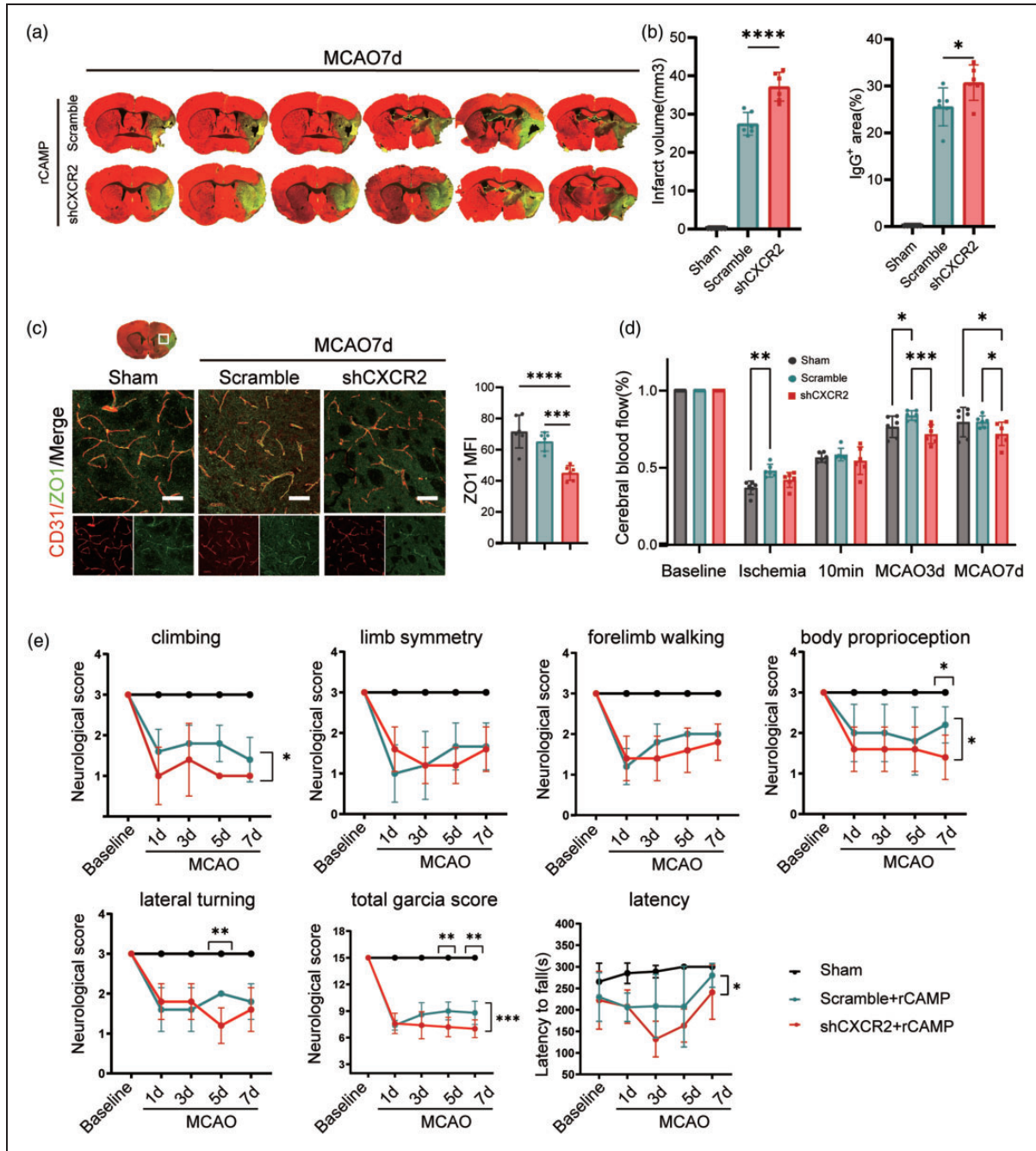


Figure 5. Knockdown of CXCR2 increases infarct volume and impairs neurological recovery after ischemic stroke. (a) Representative MAP2 staining of brain infarct and endogenous mouse IgG staining of BBB leakage of scramble-shRNA and CXCR2-shRNA group 7 days after MCAO. (b) Quantification of infarct volume and endogenous IgG positive area of scramble-shRNA and CXCR2-shRNA group 7 days after MCAO (n = 6 per group, one-way ANOVA with Bonferroni multiple comparisons test). (c) Representative confocal images and quantification of tight junction protein ZO-1 and CD31 in the penumbra regions of scramble-shRNA and CXCR2-shRNA group 7 days after MCAO or sham operation. Scale bar, 50µm. Quantification of ZO-1 MFI of CD31⁺ cerebral endothelial cells. (d) Quantitative measurements of CBF of sham, scramble-shRNA and CXCR2-shRNA group at indicated timepoints. Results were expressed as percent change from baseline (n = 6 per group, one-way ANOVA with Bonferroni multiple comparisons test) and (e) Sensorimotor function was assessed using Garcia score and rotarod for scramble-shRNA and CXCR2-shRNA group after MCAO and sham group (n = 6 per group, two-way repeated measures ANOVA and post hoc Dunnett’s test). All data are presented as means ± SD, *P < 0.01, **P < 0.001, ***P < 0.0001.

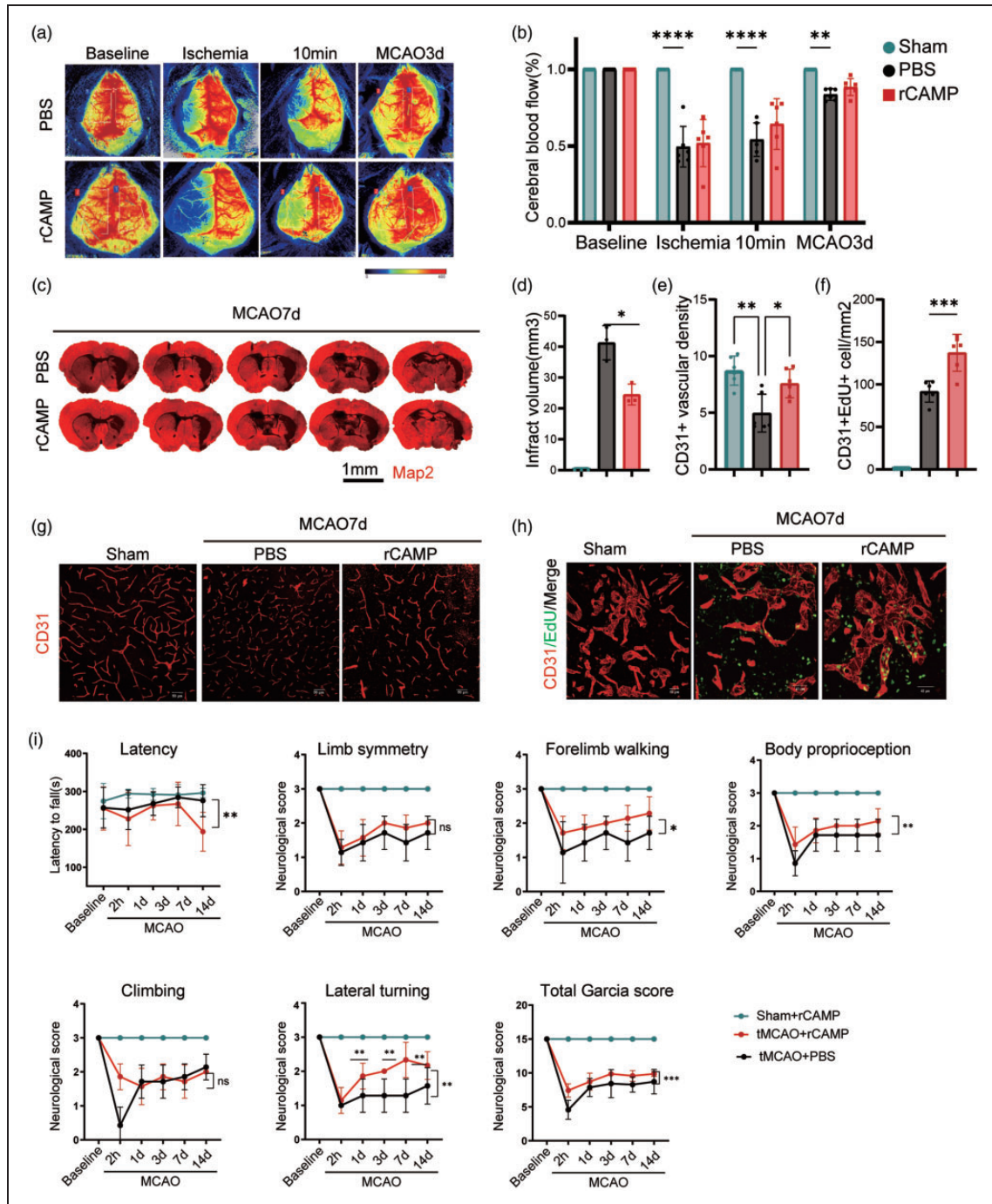


Figure 6. rCAMP promotes cerebral EC proliferation and neurological repair after ischemic stroke. (a–b) Representative images and quantitative measurements of CBF of mice treated with rCAMP or PBS before MCAO (baseline), during ischemia, 10 minutes and 3d after reperfusion ($n = 6$ per group, unpaired Student's *t*-test). (c–d) Representative MAP2 staining of brain infarct and quantification of infarct volume for PBS or rCAMP treated mice 7 days after MCAO ($n = 3$ per group, unpaired Student's *t*-test). All data are presented as means \pm SD, * $P < 0.05$. (e) Quantification of CD31⁺ vascular density in the penumbra regions of PBS or rCAMP treated mice 7 days after MCAO or sham surgery ($n = 6$ per group, one-way ANOVA with Bonferroni multiple comparisons test). (f) Quantification of CD31⁺ EdU⁺ cells in the penumbra regions of PBS or rCAMP treated mice 7 days after MCAO or sham operation ($n = 6$ per group, one-way ANOVA with Bonferroni multiple comparisons test). (g) Representative images of immunofluorescence for CD31⁺ cerebral endothelial cells in the penumbra regions of rCAMP or PBS treated mice 7 days after MCAO or sham operation. Scale bar, 50µm. (h) Representative confocal images of EdU and CD31 double immunostaining in the penumbra regions of PBS or rCAMP treated mice 7 days after MCAO or sham surgery. Scale bar, 40µm and (i) Sensorimotor function was assessed using Garcia score, rotarod, and foot-fault test for PBS or rCAMP treated mice ($n = 6$ per group, two-way repeated measures ANOVA and post hoc Dunnett's test). All data are presented as means \pm SD, * $P < 0.05$, ** $P < 0.01$, *** $P < 0.001$, ns, no significance.

other roles in the early stage of ischemic stroke. Further studies are warranted to identify the signaling activated by CAMP leading to proliferation of endothelial cells.

In summary, the current study demonstrates that neutrophil-derived CAMP significantly enhances cerebral angiogenesis and improved neurological functions in the late phase of ischemic stroke. Our findings may shed light on an endogenous neuroprotective mechanism of neutrophils, from which granular proteins released not only play a role in bactericidal function and tissue damage, but also promote tissue repair during the late phase of stroke. Furthermore, this study suggests that CAMP could serve as an attractive therapeutic target to improve neurovascular recovery in the pursuit of better neurological function after stroke.

Funding

The author(s) disclosed receipt of the following financial support for the research, authorship, and/or publication of this article: P.L. is supported by the National Natural Science Foundation of China (NSFC, 91957111, 81971096, 82061130224, M-0671), New Frontier Technology Joint Research (SHDC12019102) and Ward Building Project for Demonstration and Research sponsored by Shanghai Shenkang Hospital Development Center, Shanghai Municipal Education Commission-Gaofeng Clinical Medical Grant Support (20181805), “Shuguang Program” supported by Shanghai Education Development Foundation and Shanghai Municipal Education Commission (20SG17), “Shanghai Outstanding Academic Leaders Program” from Shanghai Municipal Science and Technology Committee (20XD1422400), the Newton Advanced Fellowship grant provided by the UK Academy of Medical Sciences (NAF\R11\1010) and the Innovative Research Team of High-level Local Universities in Shanghai (SHSMU-ZLCX20211602).

Data availability

All datasets are included in the manuscript and supporting information. Original data are available upon request.

Declaration of conflicting interests

The author(s) declared no potential conflicts of interest with respect to the research, authorship, and/or publication of this article.

Authors' contributions

WX, TH and GL performed the experiments, WX, TH and GL generate the idea and design the experiments. WX, HT, YZ, WC, CC, YL collected the data and performed the analysis. WX and GL wrote the manuscript, PL supervised the project and revised the manuscript.

Supplementary material

Supplemental material for this article is available online.

ORCID iD

Peiyang Li  <https://orcid.org/0000-0002-5721-9914>

References

1. Wu S, Wu B, Liu M, China Stroke Study Collaboration, et al. Stroke in China: advances and challenges in epidemiology, prevention, and management. *Lancet Neurol* 2019; 18: 394–405.
2. Krupinski J, Kaluza J, Kumar P, et al. Role of angiogenesis in patients with cerebral ischemic stroke. *Stroke* 1994; 25: 1794–1798.
3. Ma Y, Yang S, He Q, et al. The role of immune cells in post-stroke angiogenesis and neuronal remodeling: the known and the unknown. *Front Immunol* 2021; 12: 784098.
4. Phillipson M and Kubes P. The healing power of neutrophils. *Trends Immunol* 2019; 40: 635–647.
5. Chen C, Huang T, Zhai X, et al. Targeting neutrophils as a novel therapeutic strategy after stroke. *J Cereb Blood Flow Metab* 2021; 41: 2150–2161.
6. Li Y, Zhu ZY, Huang TT, et al. The peripheral immune response after stroke – a double edge sword for blood-brain barrier integrity. *CNS Neurosci Ther* 2018; 24: 1115–1128.
7. Mai N, Prifti V, Kim M, et al. Characterization of neutrophil-neuronal co-cultures to investigate mechanisms of post-ischemic immune-mediated neurotoxicity. *J Neurosci Methods* 2020; 341: 108782.
8. Neumann J, Sauerzweig S, Röncke R, et al. Microglia cells protect neurons by direct engulfment of invading neutrophil granulocytes: a new mechanism of CNS immune privilege. *J Neurosci* 2008; 28: 5965–5975.
9. Ardi VC, Kupriyanova TA, Deryugina EI, et al. Human neutrophils uniquely release TIMP-free MMP-9 to provide a potent catalytic stimulator of angiogenesis. *Proc Natl Acad Sci U S A* 2007; 104: 20262–20267.
10. Christoffersson G, Vågesjö E, Vandooren J, et al. VEGF-A recruits a proangiogenic MMP-9-delivering neutrophil subset that induces angiogenesis in transplanted hypoxic tissue. *Blood* 2012; 120: 4653–4662.
11. Aldabbous L, Abdul-Salam V, McKinnon T, et al. Neutrophil extracellular traps promote angiogenesis: evidence from vascular pathology in pulmonary hypertension. *Arterioscler Thromb Vasc Biol* 2016; 36: 2078–2087.
12. Jickling GC, Liu D, Ander BP, et al. Targeting neutrophils in ischemic stroke: translational insights from experimental studies. *J Cereb Blood Flow Metab* 2015; 35: 888–901.
13. Perez-de-Puig I, Miró-Mur F, Ferrer-Ferrer M, et al. Neutrophil recruitment to the brain in mouse and human ischemic stroke. *Acta Neuropathol* 2015; 129: 239–257.
14. Winneberger J, Schöls S, Lessmann K, et al. Platelet endothelial cell adhesion molecule-1 is a gatekeeper of neutrophil transendothelial migration in ischemic stroke. *Brain Behav Immun* 2021; 93: 277–287.
15. Minns D, Smith KJ, Alessandrini V, et al. The neutrophil antimicrobial peptide cathelicidin promotes Th17 differentiation. *Nat Commun* 2021; 12: 1285.

16. Dorschner RA, Pestonjamas VP, Tamakuwala S, et al. Cutaneous injury induces the release of cathelicidin antimicrobial peptides active against group A Streptococcus. *J Invest Dermatol* 2001; 117: 91–97.
17. Koczulla R, von Degenfeld G, Kupatt C, et al. An angiogenic role for the human peptide antibiotic LL-37/hCAP-18. *J Clin Invest* 2003; 111: 1665–1672.
18. Salvado MD, Di Gennaro A, Lindbom L, et al. Cathelicidin LL-37 induces angiogenesis via PGE2-EP3 signaling in endothelial cells, in vivo inhibition by aspirin. *Arterioscler Thromb Vasc Biol* 2013; 33: 1965–1972.
19. Li J, Post M, Volk R, et al. PR39, a peptide regulator of angiogenesis. *Nat Med* 2000; 6: 49–55.
20. Chon JH, Houston MM, Xu C, et al. PR-39 coordinates changes in vascular smooth muscle cell adhesive strength and locomotion by modulating cell surface heparan sulfate-matrix interactions. *J Cell Physiol* 2001; 189: 133–143.
21. Percie Du Sert N, Hurst V, Ahluwalia A, et al. The ARRIVE guidelines 2.0: updated guidelines for reporting animal research. *J Cereb Blood Flow Metab* 2020; 40: 1769–1777.
22. Leventhal JM, Forsyth BW, Qi K, et al. Maltreatment of children born to women who used cocaine during pregnancy: a population-based study. *Pediatrics* 1997; 100: E7.
23. Pinho-Ribeiro FA, Baddal B, Haarsma R, et al. Blocking neuronal signaling to immune cells treats streptococcal invasive infection. *Cell* 2018; 173: 1083–1097.e22.
24. Bei Y, Pan LL, Zhou Q, et al. Cathelicidin-related antimicrobial peptide protects against myocardial ischemia/reperfusion injury. *BMC Med* 2019; 17: 42.
25. Wu Y, Zhang Y, Zhang J, et al. Cathelicidin aggravates myocardial ischemia/reperfusion injury via activating TLR4 signaling and P2X(7)R/NLRP3 inflammasome. *J Mol Cell Cardiol* 2020; 139: 75–86.
26. Norman P. Evidence on the identity of the CXCR2 antagonist AZD-5069. *Expert Opin Ther Pat* 2013; 23: 113–117.
27. Bhattacharya A, Wang Q, Ao H, et al. Pharmacological characterization of a novel centrally permeable P2X7 receptor antagonist: JNJ-47965567. *Br J Pharmacol* 2013; 170: 624–640.
28. Wang Y, Tian M, Tan J, et al. Irisin ameliorates neuroinflammation and neuronal apoptosis through integrin $\alpha V\beta 5$ /AMPK signaling pathway after intracerebral hemorrhage in mice. *J Neuroinflammation* 2022; 19: 1–20.
29. Tasca CI, Dal-Cim T and Cimarosti H. In vitro oxygen-glucose deprivation to study ischemic cell death. *Methods Mol Biol* 2015; 1254: 197–210.
30. Mao L, Li P, Zhu W, et al. Regulatory T cells ameliorate tissue plasminogen activator-induced brain haemorrhage after stroke. *Brain* 2017; 140: 1914–1931.
31. Gupta S and Kaplan MJ. The role of neutrophils and NETosis in autoimmune and renal diseases. *Nat Rev Nephrol* 2016; 12: 402–413.
32. Pircher J, Czermak T, Ehrlich A, et al. Cathelicidins prime platelets to mediate arterial thrombosis and tissue inflammation. *Nat Commun* 2018; 9: 1523.
33. Zheng K, Lin L, Jiang W, et al. Single-cell RNA-seq reveals the transcriptional landscape in ischemic stroke. *J Cereb Blood Flow Metab* 2022; 42: 56–73.
34. Jakkamsetti V, Scudder W, Kathote G, et al. Quantification of early learning and movement substructure predictive of motor performance. *Sci Rep* 2021; 11: 1–14.
35. Elssner A, Duncan M, Gavrilin M, et al. A novel P2X7 receptor activator, the human cathelicidin-derived peptide LL37, induces IL-1 β processing and release. *J Immunol* 2004; 172: 4987–4994.
36. Minns D, Smith KJ, Alessandrini V, et al. The neutrophil antimicrobial peptide cathelicidin promotes Th17 differentiation. *Nat Commun* 2021; 12: 1285.
37. Mookherjee N, Lippert DND, Hamill P, et al. Intracellular receptor for human host defense peptide LL-37 in monocytes. *J Immunol* 2009; 183: 2688–2696.
38. Tjabringa GS, Ninaber DK, Drijfhout JW, et al. Human cathelicidin LL-37 is a chemoattractant for eosinophils and neutrophils that acts via formyl-peptide receptors. *Int Arch Allergy Immunol* 2006; 140: 103–112.
39. Vandamme D, Landuyt B, Luyten W, et al. A comprehensive summary of LL-37, the factotum human cathelicidin peptide. *Cell Immunol* 2012; 280: 22–35.
40. Yang D, Chen Q, Schmidt AP, et al. LL-37, the neutrophil granule- and epithelial cell-derived cathelicidin, utilizes formyl peptide receptor-like 1 (FPRL1) as a receptor to chemoattract human peripheral blood neutrophils, monocytes, and T cells. *J Exp Med* 2000; 192: 1069–1074.
41. Zhang Z, Cherryholmes G, Chang F, et al. Evidence that cathelicidin peptide LL-37 may act as a functional ligand for CXCR2 on human neutrophils. *Eur J Immunol* 2009; 39: 3181–3194.
42. Cole AM, Shi J, Ceccarelli A, et al. Inhibition of neutrophil elastase prevents cathelicidin activation and impairs clearance of bacteria from wounds. *Blood* 2001; 97: 297–304.
43. Steinstraesser L, Lam MC, Jacobsen F, et al. Skin electroporation of a plasmid encoding hCAP-18/LL-37 host defense peptide promotes wound healing. *Mol Ther* 2014; 22: 734–742.
44. Ter Schiphorst A, Charron S, Hassen WB, et al. Tissue no-reflow despite full recanalization following thrombectomy for anterior circulation stroke with proximal occlusion: a clinical study. *J Cereb Blood Flow Metab* 2021; 41: 253–266.
45. Ng FC, Churilov L, Yassi N, et al. Prevalence and significance of impaired microvascular tissue reperfusion despite macrovascular angiographic reperfusion (no-reflow). *Neurology* 2022; 98: e790–e801.
46. Hatakeyama M, Ninomiya I and Kanazawa M. Angiogenesis and neuronal remodeling after ischemic stroke. *Neural Regen Res* 2020; 15: 16–19.
47. Chopp M, Zhang ZG and Jiang Q. Neurogenesis, angiogenesis, and MRI indices of functional recovery from stroke. *Stroke* 2007; 38: 827–831.
48. Kufareva I, Gustavsson M, Zheng Y, et al. What do structures tell us about chemokine receptor function and antagonism? *Annu Rev Biophys* 2017; 46: 175–198.

49. Reutershan J, Morris MA, Burcin TL, et al. Critical role of endothelial CXCR2 in LPS-induced neutrophil migration into the lung. *J Clin Invest* 2006; 116: 695–702.
50. Miyake M, Goodison S, Urquidi V, et al. Expression of CXCL1 in human endothelial cells induces angiogenesis through the CXCR2 receptor and the ERK1/2 and EGF pathways. *Lab Invest* 2013; 93: 768–778.
51. Schraufstatter IU, Chung J and Burger M. IL-8 activates endothelial cell CXCR1 and CXCR2 through rho and rac signaling pathways. *Am J Physiol Lung Cell Mol Physiol* 2001; 280: L1094–L1103.
52. DeLeon-Pennell KY, Mouton AJ, Ero OK, et al. LXR/RXR signaling and neutrophil phenotype following myocardial infarction classify sex differences in remodeling. *Basic Res Cardiol* 2018; 113: 40.
53. Smith JM, Shen Z, Wira CR, et al. Effects of menstrual cycle status and gender on human neutrophil phenotype. *Am J Reprod Immunol* 2007; 58: 111–119.
54. Aomatsu M, Kato T, Kasahara E, et al. Gender difference in tumor necrosis factor- α production in human neutrophils stimulated by lipopolysaccharide and interferon- γ . *Biochem Biophys Res Commun* 2013; 441: 220–225.